

3 Cemented Backfill Pillar Performance

3.1 Problem Statement

This example studies the failure mode of cemented backfill pillars, which are represented as a Mohr-Coulomb material. The pillar is three-dimensional in geometry, measuring 75 m in height by 27 m in length and 15 m in width. The material properties of the fill are

density (ρ)	2100 kg/m ³
bulk modulus (K)	110 MPa
shear modulus (G)	37 MPa
cohesion (c)	0.1 MPa
friction angle (ϕ)	35°
tensile strength ($\frac{c}{\tan\phi}$)	0.14 MPa

3.2 Modeling Procedure

The analysis is made along a two-dimensional longitudinal section through the pillar center. The problem geometry and analysis plane are illustrated in [Figure 3.1](#). A sliding interface is used along one of the orebody-sandfill contacts to allow downward settling of the sand during collapse. The boundary at the fill-ore contact (which is to be excavated) is given a roller boundary, and the right-hand boundary is fixed in the x - and y -directions; the top is free ([Figure 3.1](#)).

The modeling sequence is as follows. First, the gravity stresses are allowed to develop in the sandfill, and forces equilibrate across the interface. This is done elastically so that the fill will not yield. At equilibrium, displacements are reset, cohesion is set to the proper value, and vertical retreat mining is simulated by removing the x -direction fix along the left-face boundary in small increments that simulate the blast height (6 m). The x -displacement history is used to evaluate whether the system is coming to equilibrium at each step. Excavation is continued until active collapse of the pillar occurs.

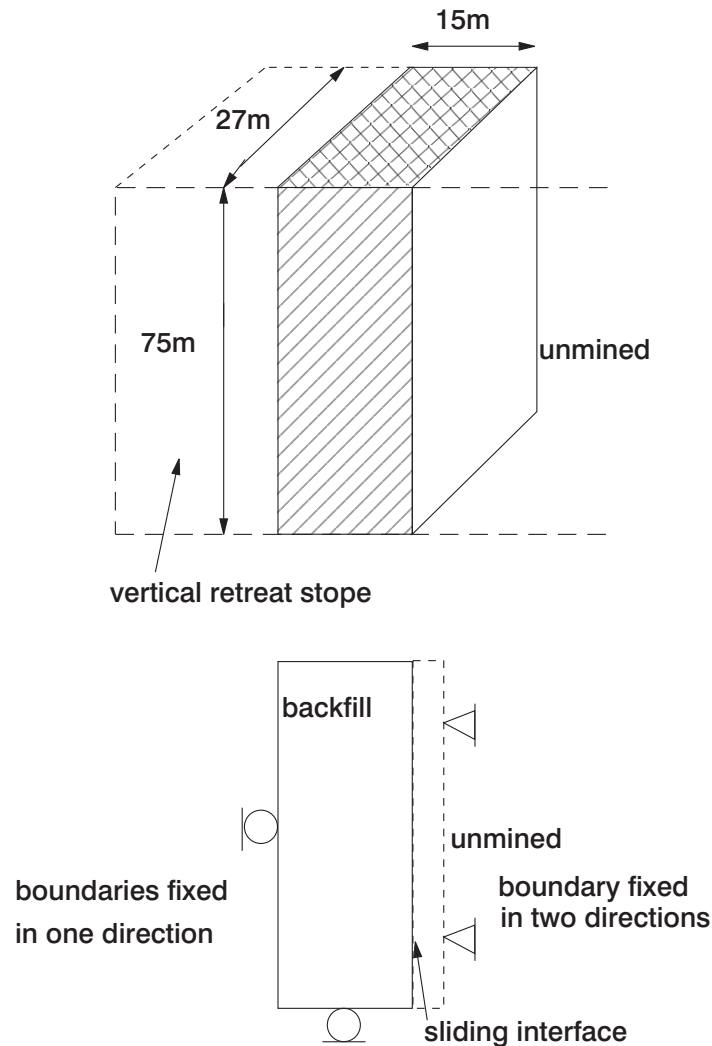


Figure 3.1 *Schematic illustrating true three-dimensional backfill pillar geometry and two-dimensional representation*

3.3 Results

Figures 3.2 through 3.7 show displacement vectors in the model at different blast heights. The model comes to equilibrium for the first three blast heights (6 m, 12 m and 18 m), as indicated by Figures 3.2 through 3.5. Only a small localized displacement is shown in each of these figures. Note that after excavation of the 18 m blast height, the zones nearest to the left-face boundary fail in tension. These zones are deleted in order to remove elements that will produce a bad zone geometry as the excavation continues. The model is still in equilibrium after these zones are deleted; Figures 3.4 and 3.5 show displacements before and after tension-failed zones were deleted. For the

first three stages (6 m, 12 m and 18 m blast heights), the model can be brought to equilibrium after each excavation is made by using the **SOLVE** command.

At the fourth blast height (24 m), collapse of the pillar begins to occur. The failure is shown by the large region of downward movement that is shown in Figure 3.6. The failure is even more evident at the 30 m blast height, as shown by Figure 3.7. The deformed boundary and plasticity states at collapse of the pillar are shown in Figure 3.8. A history of x -displacement at the left-face boundary is shown in Figure 3.9. This gridpoint history is reset at the fourth blast height, and indicates that the model reaches equilibrium at this stage and collapses in the next.

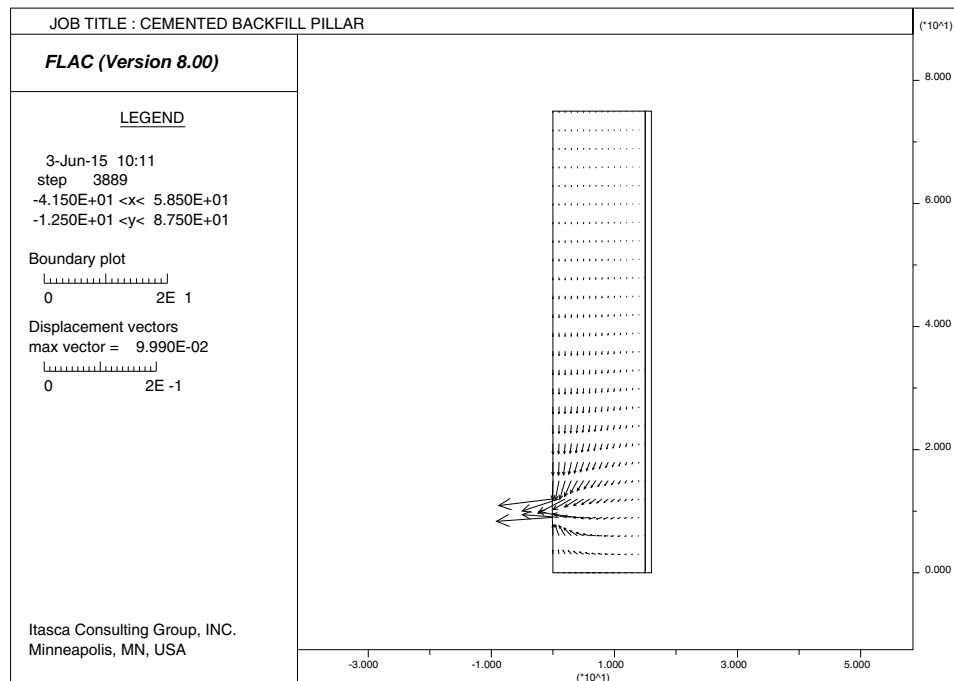


Figure 3.2 Displacement vectors at 6 m blast height

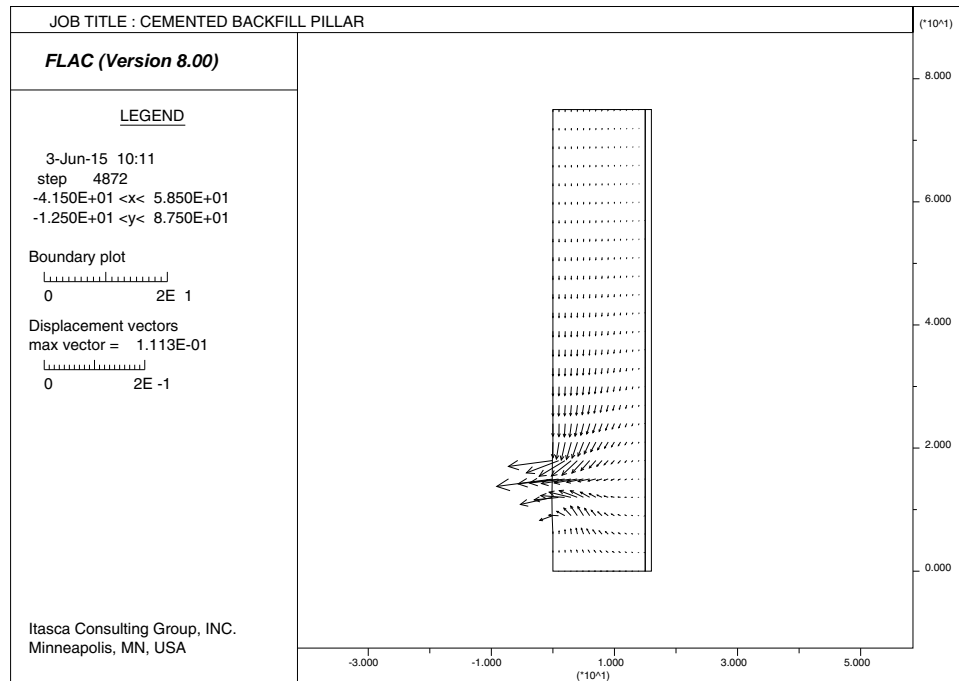


Figure 3.3 Displacement vectors at 12 m blast height

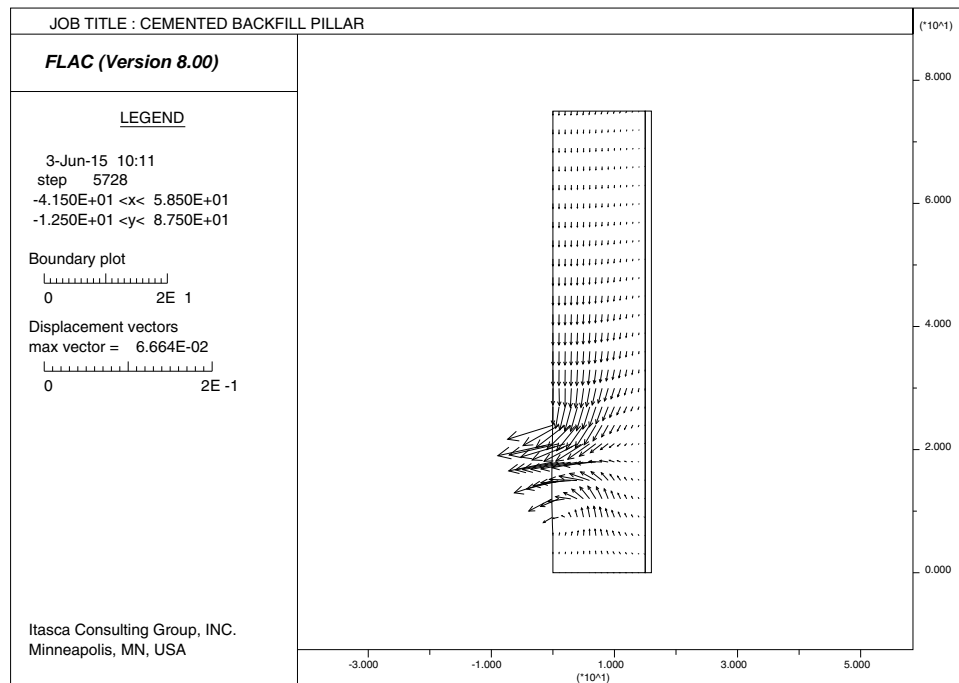


Figure 3.4 Displacement vectors at 18 m blast height

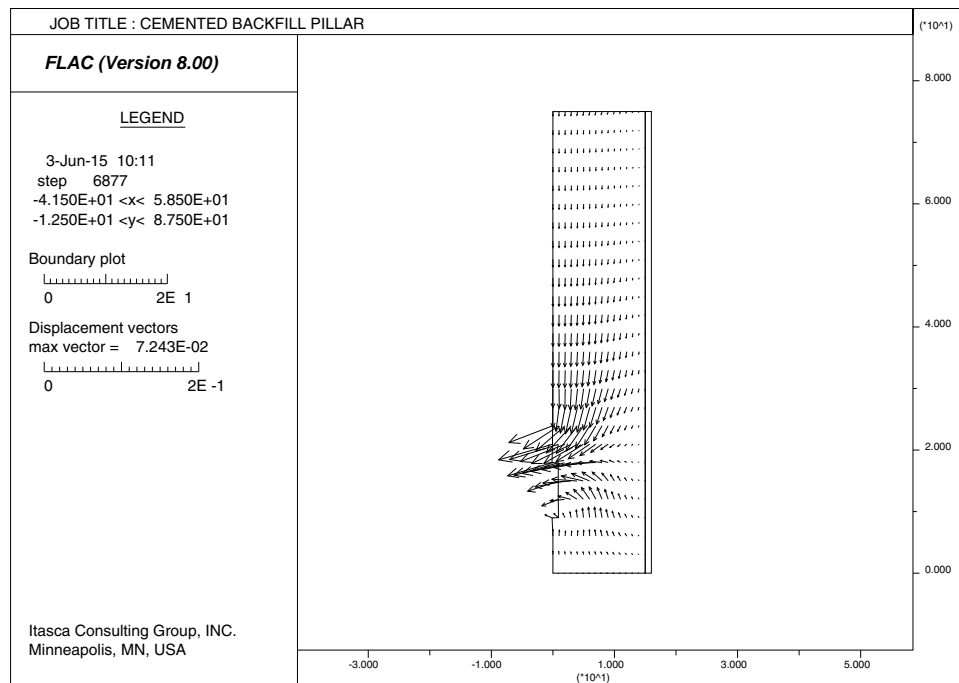


Figure 3.5 Displacement vectors at 18 m blast height (tension failed zones removed)

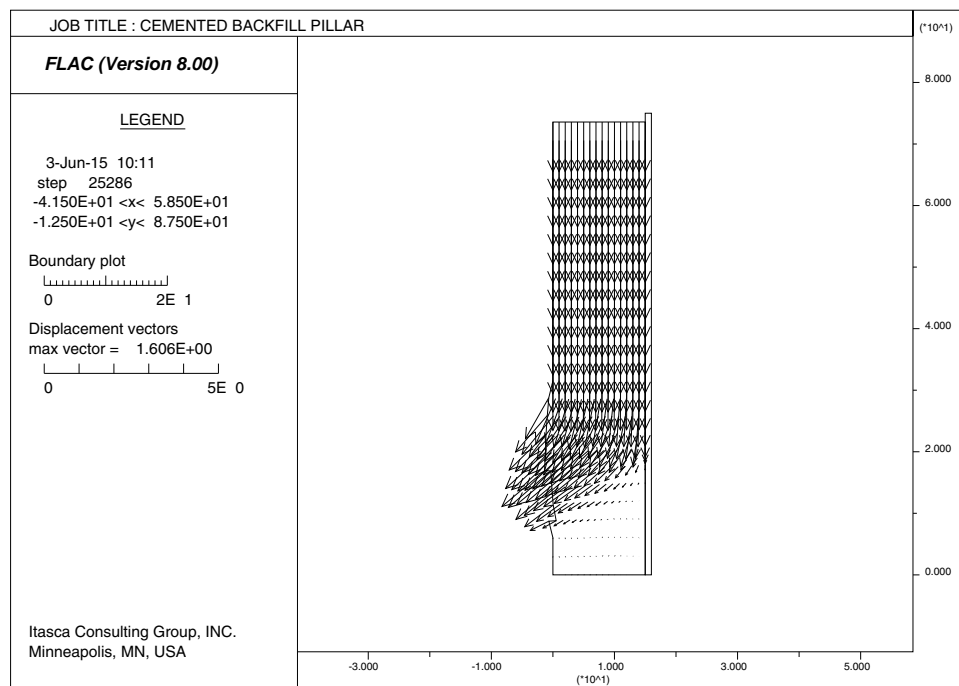


Figure 3.6 Displacement vectors at 24 m blast height

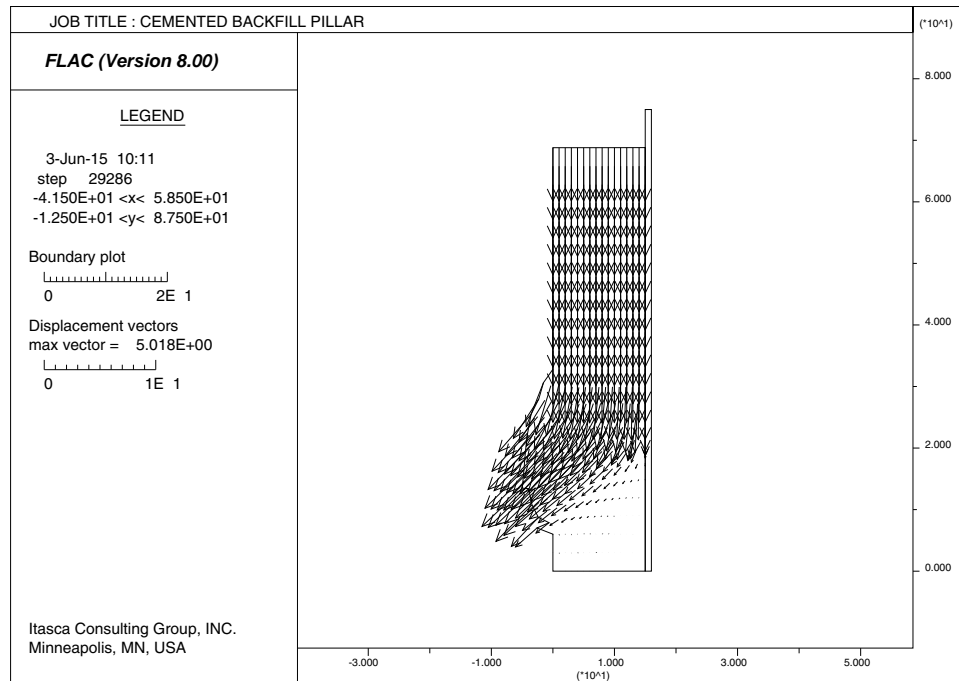


Figure 3.7 Displacement vectors at 30 m blast height

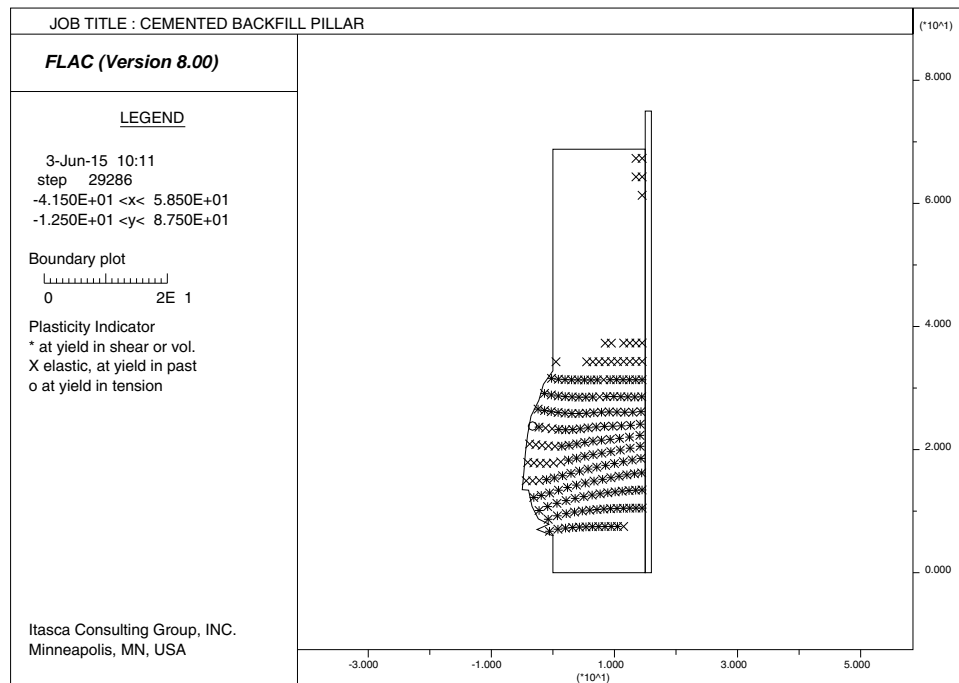


Figure 3.8 Plasticity indicators and deformed grid at 30 m blast height

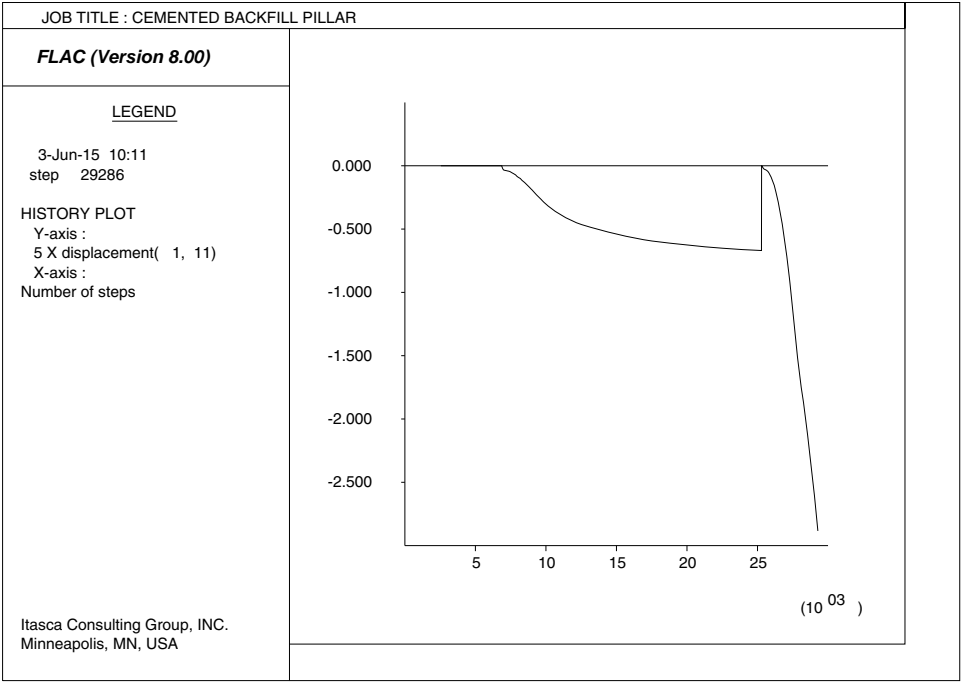


Figure 3.9 *History of x-displacement at 30 m height on pillar wall*

